An exact analysis of spontaneous emission by a single two level atom in the rotating wave approximation II. Numerical results

1972 J. Phys. A: Gen. Phys. 5 1601

(http://iopscience.iop.org/0022-3689/5/11/008)

J. Phys. A: Gen. Phys., Vol. 5, November 1972. Printed in Great Britain.

An exact analysis of spontaneous emission by a single two level atom in the rotating wave approximation II. Numerical results

S SWAIN

Department of Applied Mathematics and Theoretical Physics, The Queen's University of Belfast, Belfast BT7 1NN, UK

MS received 18 May 1972

Abstract. The problem considered is that of spontaneous emission by a single, two level atom which interacts with N modes of the electromagnetic field in the electric dipole, rotating wave approximation. The equations derived in a preceeding paper are solved numerically for $N = 4, 5, 10, 11, 20, 21$, and 201 to find the eigenvalues and various time dependent properties of the system. The connection between our approach and conventional Wigner–Weisskopf theory is discussed.

1. Introduction

The methods set out in two previous publications (Swain 1972a, 1972b) have been shown (Swain 1972c, to be referred to as I) to lead to an exact solution of the problem of spontaneous emission by a single two level atom which interacts with N modes of the electromagnetic field in the electric dipole, rotating wave approximation. In I we gave analytic results for the cases $N = 1$, 2, and 3. In this paper we present and discuss the results of numerical solutions of our equations made with the aid of an electronic computer for various values of N from 4 to 201.

The model Hamiltonian we consider is

$$H = \sum_{\lambda=1}^{N} a_\lambda^\dagger a_\lambda \omega_\lambda + \sigma^3 \omega_0 + \sum_{\lambda=1}^{N} (g_\lambda a_\lambda \sigma^+ + g_\lambda^* a_\lambda^\dagger \sigma^-) \tag{1}$$

where $a_\lambda^\dagger$ creates a photon in the mode λ whose frequency is ω_λ, σ^3, σ^+ and σ^- are spin one-half operators, ω_0 is the energy separation of the two atomic levels, and g_λ is the coupling constant between the atom and field modes. It is given explicitly by the relation

$$g_\lambda = -\mathrm{i}(2\pi\omega_\lambda V)^{-1/2} \boldsymbol{d} \cdot \boldsymbol{u}_\lambda \tag{2}$$

where V is the volume of the system, $\boldsymbol{d}$ the dipole matrix element, and $\boldsymbol{u}_\lambda$ is the normal mode function of the cavity for the mode λ evaluated at the position of the atom. We use throughout a system of units in which $\hbar = 1$. (1) describes a system of N electromagnetic modes interacting with a single two level atom in the electric dipole, rotating wave approximation.

In § 2 we manipulate the equations derived in I into a form suitable for numerical computation, and in § 3 we use these equations to calculate the energy eigenvalues of

the system. We also derive approximate expressions for these eigenvalues. In § 4 we discuss the connection between our work, and that of Davidson and Kozak, and Weisskopf and Wigner. This discussion emphasizes the connection between the Wigner–Weisskopf approach and the rotating wave approximation. In § 5 we discuss the time dependent behaviour of the atom and the field as the system evolves from an initial state with the atom excited and no photons present.

2. The numerical calculation

It is convenient for the numerical work to work with dimensionless variables. We first of all assume that $g_\lambda = g$, a constant independent of the mode λ. As we have mentioned in I, this is an approximation—most commonly g_λ is taken to be proportional to $(\omega_\lambda)^{1/2}$, but as this form leads to difficulties in the infinite mode case (the ultraviolet divergence) many other functional dependences on ω_λ are frequently assumed (including the one we have chosen here). We must emphasize that it is not essential for the numerical work to make this assumption. The particular advantage of taking g_λ to be a constant for our purposes is that it enables us to write our equations in a form independent of the magnitude of $|g|$. With the particular mode frequency scheme we choose, this enables us to give results which depend only on the total number of interacting modes and the energy separation between adjacent modes.

In I we showed that the eigenvalues of (1) appropriate to spontaneous emission were

$$E(q) = \tfrac{1}{2}\omega_0 + q \tag{3}$$

where q is determined by equation (20) of I. (We will write the equations of I as, eg I20.) We also gave expressions for $P_0(t)$, the probability that an atom will be in its excited state at time t (I37), and $p_n(t)$, the probability that there will be a photon in the mode λ at time t (I35). Both these probabilities are conditional on the atom being in its excited state at $t = 0$ with no photons present. Our principle objective in this paper is to calculate q, $P_0(t)$ and $p_n(t)$ for different values of N (the number of modes).

If we define the dimensionless variables

$$Q = q/|g| \tag{4}$$

$$\Omega_\lambda = \omega_\lambda/|g| \tag{5}$$

and

$$\Omega_0 = \omega_0/|g| \tag{6}$$

then we can write (I20), (I24), (I37) and (I35) as

$$Q - \sum_{\lambda=1}^{N} \frac{1}{Q-\Omega_{\lambda,0}} = 0 \tag{7}$$

$$|B_Q(0)|^2 = \left(1 + \sum_{\lambda=1}^{N} \frac{1}{(Q-\Omega_{\lambda,0})^2}\right)^{-1} \tag{8}$$

$$P_0(\tau) = \left|\sum_Q |B_Q(0)|^2 \exp(-\mathrm{i}Q\tau)\right|^2 \tag{9}$$

and

$$p_\lambda(\tau) = \left|\sum_Q \frac{|B_Q(0)|^2}{Q-\Omega_{\lambda,0}} \exp(-\mathrm{i}Q\tau)\right|^2 \tag{10}$$

where $\Omega_{\lambda,0} \equiv \Omega_\lambda - \Omega_0$ and $\tau \equiv |g|t$ is a dimensionless time variable. In (8), (9) and (10) Q is understood to be a root of (7). It is evident that these equations do not depend explicitly on $|g|$.

We must now decide our mode frequency scheme. In a general discussion such as this, there seems no reason to deviate from a symmetric disposition of the mode frequencies about the atomic energy. Accordingly, we consider two schemes in which the mode energies are evenly and symmetrically placed about ω_0:

$$\omega_{\lambda,0} = n\delta \begin{cases} n = 0, \pm 1, \pm 2, \ldots, \pm \tfrac{1}{2}N & \text{for } N \text{ even} \\ n = \pm \tfrac{1}{2}, \pm \tfrac{3}{2}, \pm \ldots \pm \tfrac{1}{2}N & \text{for } N \text{ odd.} \end{cases} \tag{11}$$

Here N is always integral, and we note that now the total number of modes is $N+1$. In the first case (N even) there is always one mode on resonance with the atom, in the second case (N odd) there never is. In terms of dimensionless variables we have

$$\Omega_{\lambda,0} = n\Delta \tag{12}$$

where

$$\Delta = \delta/|g|. \tag{13}$$

The condition

$$\omega_\lambda = \omega_0 + n\delta \geqslant 0$$

must be satisfied for all n. This implies

$$\frac{\delta}{\omega_0} = \frac{\Delta}{\Omega_0} \leqslant \frac{2}{N} \tag{14}$$

for N odd or even. Thus δ (or Δ) must be less than the limits specified for our equations to be meaningful.

Using (11) our eigenvalue equation (7) may be written

$$Q - \sum_n \frac{1}{Q - n\Delta} = 0 \tag{15}$$

where the sum over n extends from $n = -N/2$ to $+N/2$. If we write $-Q$ for Q, it is clear that $-Q$ satisfies (15) if Q does. Also, for the case N odd, it can be seen that $Q = 0$ is a solution. Thus the roots of (15) are

$$\pm Q_1, \pm Q_2, \pm Q_3, \ldots \pm Q_{\frac{1}{2}N+1} \qquad \text{for } N \text{ even}$$

and

$$0, \pm Q_{1/2}, \pm Q_{3/2}, \ldots \pm Q_{\frac{1}{2}N} \qquad \text{for } N \text{ odd.}$$

In either case, the total number of roots is $N+2$. Consequently, we may write

$$|B_Q(0)|^2 = |B_{-Q}(0)|^2 = \left(1 + \sum_n \frac{1}{(Q - n\Delta)^2}\right)^{-1} \tag{16}$$

and

$$p_n(\tau) = \left| \sum_Q \frac{|B_Q(0)|^2}{Q - n\Delta} \exp(-iQ\tau) \right|^2 . \tag{17}$$

corresponding to the probability of the mode of frequency $\Omega_0 + n\Delta$ being occupied.

Because of the symmetry of Q and our energy level scheme we have the property $p_n(\tau) = p_{-n}(\tau)$. Equations (15), (16), (17) and (9) provide the basis for our numerical work. We note that these equations depend only on N, Δ and τ, and do not involve $|g|$ or ω_0 explicitly.

3. The energy eigenvalues

We have solved the eigenvalue problem (15) for the Q numerically for various values of N and Δ. The results have a different structure according to whether N is odd or even (corresponding to the different energy level schemes previously described). We

Table 1. The eigenvalues $Q_n(N, \Delta)$. Only the positive roots are given (since $-Q$ is also an eigenvalue) and the roots are arranged in order of increasing magnitude. Also shown (between the broken lines) are approximate expressions for the first and last eigenvalues.

Number of modes $(N+1)$	$\Delta = 0{\cdot}1$	$\Delta = 0{\cdot}5$	$\Delta = 1{\cdot}0$	$\Delta = 2{\cdot}0$	$\Delta = 10{\cdot}0$
5	0·0543	0·2647	0·4901	0·7636	0·9876
$(N = 4)$	0·1643	0·8027	1·4848	2·4374	10·0998
$\sqrt{5} = 2{\cdot}236$	2·2405	2·3528	2·7487	4·2984	20·0504
$\Delta(N/2)+1/(N/2)\Delta$	—	2·00	2·50	4·20	20·050
11	0·0519	0·2529	0·4698	0·7418	0·9856
$(N = 10)$	0·1557	0·7594	1·4123	2·3979	10·0993
	0·2598	1·2681	2·3626	4·2471	20·0501
	0·3646	1·7821	3·3245	6·1758	30·0334
	0·4711	2·3099	4·3038	8·1368	40·0251
$\sqrt{11} = 3{\cdot}317$	3·3318	3·7403	5·3506	10·1150	50·0201
$\Delta(N/2)+1/\Delta(N/2)$	—	2·90	5·20	10·10	50·02
21	0·0509	0·2485	0·4623	0·7336	0·9848
$(N = 20)$	0·1528	0·7456	1·3906	2·3852	10·0992
	0·2547	1·2430	2·3285	4·2365	20·0500
	0·3567	1·7408	3·2780	6·1666	30·0334
	0·4588	2·2394	4·2382	8·1278	40·0250
	0·5610	2·7392	5·2073	10·1035	50·0200
	0·6635	3·2408	6·1835	12·0869	60·0167
	0·7664	3·7455	7·1652	14·0750	70·0143
	0·8699	4·2561	8·1517	16·0662	80·0125
	0·9750	4·7816	9·1435	18·0594	90·0111
$\sqrt{21} = 4{\cdot}583$	4·6230	5·8334	10·1479	20·0547	100·0100
$\Delta(N/2)+1/(\Delta(N/2)$	—	5·20	10·10	20·05	100·010
$\frac{\Delta}{2}\left(1-\frac{\Delta^2}{\pi^2+\Delta^2}\right)$	0·050	0·2442	0·4540	0·4158	0·4540
$\left(1+\frac{\pi^2}{3\Delta^2}\right)^{-1/2}$	0·0174	0·2658	0·4829	0·7402	0·9846

discuss in detail the results for N even, and describe only briefly the results for N odd at the end of this section, as the treatment is closely analogous.

In table 1 we present the positive eigenvalues $Q_n(N, \Delta)$ for the cases where N takes the values 4, 10 and 20 (the number of modes is $N+1$) and $\Delta = 0{\cdot}1, 0{\cdot}5, 1{\cdot}0, 2{\cdot}0$ and $10{\cdot}0$. In table 2 we give the positive eigenvalues for these same values of Δ but now N takes the values 3, 9 and 19.

Table 2. The positive eigenvalues $Q_n(N, \Delta)$ for odd values of N.

Number of modes $(N+1)$	$\Delta = 0{\cdot}1$	$\Delta = 0{\cdot}5$	$\Delta = 1{\cdot}0$	$\Delta = 2{\cdot}0$	$\Delta = 10{\cdot}0$
4	0·1117	0·5449	1·0069	1·5899	5·1942
($N = 3$)	2·0031	2·0804	2·3422	3·3899	15·0672
10	0·1041	0·5079	0·9436	1·5399	5·1931
($N = 9$)	0·2085	1·0177	1·8928	3·3099	15·0666
	0·3136	1·5325	2·8530	5·2081	25·0401
	0·4205	2·0609	3·8317	7·1563	35·0287
	3·1754	3·5245	4·8945	9·1288	45·0224
	0·1020	0·4975	0·9263	1·5256	5·1927
20	0·2040	0·9952	1·8596	3·2961	15·0665
	0·3060	1·4934	2·8036	5·1963	25·0400
	0·4082	1·9922	3·7590	7·1451	35·0286
($N = 19$)	0·5105	2·4922	4·7241	9·1147	45·0222
	0·6130	2·9941	5·6972	11·0948	55·0182
	0·7160	3·4990	6·6767	13·0809	65·0154
	0·8196	4·0098	7·6616	15·0707	75·0134
	0·9247	4·5355	8·6525	17·0631	85·0118
	4·5096	5·6231	9·6578	19·0578	95·0106

We make two points about these results: (i) the values obtained for Q_n (apart from the final value for each value of N) are approximately independent of the number of modes. For example, in table 1, the first five eigenvalues for the twenty one mode case are approximately equal to the first five eigenvalues for the eleven mode case, for every value of Δ listed, and (ii) the eigenvalues (again apart from the final one) are approximately evenly spaced, and the value of the spacing is approximately Δ.

To understand these points we derive approximate expressions for $Q(N, \Delta)$.

3.1. Approximate formulae for the eigenvalues

If we make the substitution

$$Q = \Delta x \tag{18}$$

(15) can be written in the form

$$\Delta^2 x - \sum_n \frac{1}{x+n} = 0. \tag{19}$$

The functions appearing in (19) are shown for the case $N = 4$ in figure 1 for $x \geqslant 0$.

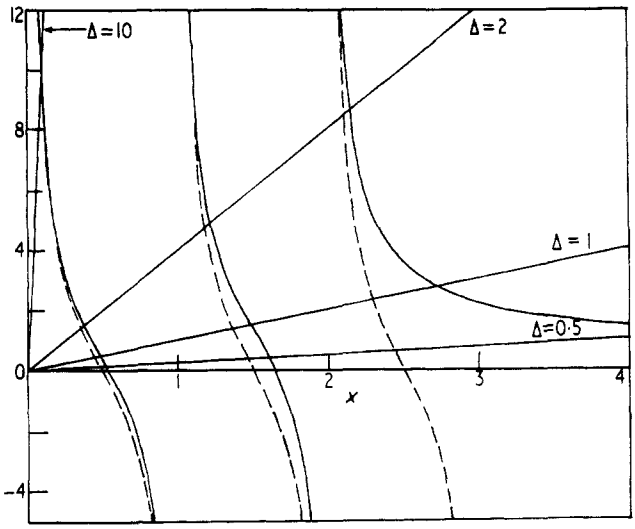

Figure 1. $y_1(x) = \Sigma_{n=-2}^{+2} 1/(x+n)$ and $y_2(x) = \Delta^2 x$ for $\Delta = 0{\cdot}5$, 1, 2 and 10 plotted for positive values of x. Shown as broken curves is $\pi \cot \pi x$.

We have plotted $y_1(x) = \Sigma_{n=-2}^{+2} 1/(x+n)$ (full curves) and on the same graph $y_2(x) = \Delta^2 x$ for $\Delta = 10$, 2, 1 and 0·5. The function $y_1(x)$ has infinite discontinuities at $x = s$, where s is an integer in the range $0 \leqslant s \leqslant N/2$. The points where $y_1(x)$ and $y_2(x)$ intersect give us the roots of (19). It is clear by inspection of figure 1 that the roots have the form

$$x_s = s + \xi \tag{20}$$

where $1 > \xi > 0$ (except possibly when $s = N/2$). Since $y_1(x)$ is infinite when x is integral and zero when x is approximately half-integral we can distinguish two extreme cases:

$$x_s \simeq s + \tfrac{1}{2} \qquad \text{if } \Delta^2(s+\tfrac{1}{2}) \ll 1$$

and

$$x_s \simeq s \qquad \text{if } \Delta^2(s+\tfrac{1}{2}) \gg 1.$$

This is evident by inspection of figure 1.

To give more accurate estimates of the roots we make use of the sum

$$\sum_{n=-\infty}^{+\infty} \frac{1}{x+n} = \pi \cot \pi x. \tag{21}$$

$\pi \cot \pi x$ has infinite discontinuities whenever x is integral and zeros whenever x is half-integral. It is shown in figure 1 plotted as broken curves. We expect that $y_1(x) \simeq \pi \cot \pi x$ for $|x| \lesssim N/2$ if N is large, but even for the case plotted in figure 1, where $N = 4$, the disparity between $y_1(x)$ and $\pi \cot \pi x$ is not extreme. For this case, if $\Delta^2 \gg 1$, it is apparent that this approximate form for $y_1(x)$ will give accurate estimates for the roots of (19).

Let us now consider the extreme cases $\Delta^2(s+\frac{1}{2}) \gg 1$ and $\Delta^2(s+\frac{1}{2}) \ll 1$ in more detail.

3.1.1. $\Delta^2(s+\frac{1}{2}) \gg 1$. Substituting (20) and (21) into (19) gives

$$\Delta^2(s+\xi) \simeq \pi \cot \pi(s+\xi) = \pi \cot \pi\xi$$

$$\simeq \pi\left(\frac{1}{\pi\xi} - \frac{\pi\xi}{3}\right) \tag{22}$$

for ξ small. This is a quadratic equation in ξ which can be solved to give

$$x_s = \frac{Q_s}{\Delta} = s\left\{\left(1-\frac{1}{2\gamma}\right) + \frac{1}{\gamma}\left(\frac{\gamma}{\Delta^2 s^2} + \frac{1}{4}\right)^{1/2}\right\} \tag{23}$$

where

$$\gamma = 1 + \frac{\pi^2}{3\Delta^2}. \tag{24}$$

For the first root Q_0 this gives

$$Q_0 = \gamma^{-1/2}. \tag{25}$$

There are two useful limiting cases:

(i) $$\Delta^2 s^2 \gg 4\gamma; \tag{26}$$

we then find

$$Q_s \simeq s\Delta + \frac{1}{s\Delta} \tag{28}$$

and thus

$$Q_{s+1} - Q_s = \Delta - \frac{1}{\Delta s(s+1)} \simeq \text{constant}. \tag{29}$$

(We note that (26) implies $s\Delta \gg 1$.) This is in accord with our previous observation that the roots Q_s seem to be separated by the amount Δ. In table 1, (28) is seen to give a good approximation to Q_s when (26) is valid.

The second case, which is only realizable when $\Delta^2 \ll 1$, is

(ii) $$\Delta^2 s^2 \ll 4\gamma. \tag{30}$$

This leads to

$$Q_s = s\Delta\left(1-\frac{1}{2\gamma}\right) + \gamma^{-1/2} \tag{31}$$

where $\gamma \gg 1$ (since $\Delta^2 \ll 1$).

Once again, this implies that the spacing between adjacent roots is approximately constant and equal to Δ.

The final root is given by (28)

$$Q_{N/2} \simeq (N/2)\Delta + \frac{1}{(N/2)\Delta} \tag{32}$$

and the condition of validity is

$$\Delta^2(N/2) \gg 1.$$

3.1.2. $\Delta^2(s+\frac{1}{2}) \ll 1$. In this case, inspection of figure 1 suggests that we write

$$x = s+\tfrac{1}{2}+\eta \tag{33}$$

where $\eta \ll 1$, (except for the case $s = N/2$). Substituting (33) and (21) into (19), we find

$$\Delta^2(s+\tfrac{1}{2}+\eta) = -\pi \tan \pi\eta \simeq -\pi^2\eta. \tag{34}$$

Hence

$$\eta = -\frac{\Delta^2(s+\frac{1}{2})}{\pi^2+\Delta^2} \tag{35}$$

and

$$x_s = \frac{Q_s}{\Delta} = (s+\tfrac{1}{2})\left(1-\frac{\Delta^2}{\pi^2+\Delta^2}\right). \tag{36}$$

As $\Delta \to 0$ we have

$$Q_s \to \Delta(s+\tfrac{1}{2}). \tag{37}$$

Inspection of table 1 shows that (37) is well satisfied for $\Delta = 0{\cdot}1$ and $0{\cdot}5$.

To estimate the final root in this case we assume $\Delta^2(N/2) \ll 1$. In this event, $x_{N/2} \simeq N/2+\zeta$ where now $\zeta \gg 1$. If we may further assume that $x_{N/2} \gg N/2$, we may approximate the sum in (19) by

$$\frac{1}{x}\sum_{n=-N/2}^{+N/2} 1 = \frac{N+1}{x}. \tag{38}$$

From (19), this must be equal to $\Delta^2 x$, and thus

$$Q_{N/2} \simeq (N+1)^{1/2}. \tag{39}$$

Thus the largest root is approximately equal to the square root of the total number of field modes.

By comparing the formulae we have derived with the exact results given in table 1 it is readily seen that these formulae give accurate estimates of the eigenvalues within their ranges of validity. To obtain approximate expressions for the eigenvalues in the intermediate range $\Delta^2(s+\frac{1}{2}) \simeq 1$, one would have to retain higher terms in the expansions of the trigonometric functions of equations (22) and (34). To facilitate comparison of the exact and approximate expressions we have evaluated in table 1 the approximate expressions (25) and (36) for the first roots, and (32) and (39) for the final roots.

Apart from (32) and (39), the approximate expressions for the eigenvalues which we have derived do not depend upon N (essentially the number of modes). This explains the first observation made at the beginning of this section that the values obtained for the eigenvalues are (apart from the final eigenvalue) approximately independent of the number of modes. Equations (28), (31), (32) and (36) account for the second observation (that the spacing of the modes is approximately equal to Δ).

Finally we consider how the results are modified for the case when N is an odd integer (which corresponds to there being an even number of modes present). The method is similar to that for N even: we make use of the relations

$$\sum_{n=-N/2}^{+N/2} \frac{1}{x+n} = \sum_{n=-(N/2+1/2)}^{+(N/2-1/2)} \frac{1}{(x+\frac{1}{2})+n}$$

$$\simeq \sum_{n=-\infty}^{+\infty} \frac{1}{(x+\frac{1}{2})+n} = -\pi \tan \pi x \tag{40}$$

and solve approximately the equation

$$\Delta^2 x + \pi \tan \pi x = 0; \tag{41}$$

this enables us to find all the roots of (19) (except the final root in the case $\Delta^2(N/2) \ll 1$). In this situation there is always a root at the origin. We consider in detail two extreme cases: $\Delta^2(s+\frac{1}{2}) \gg 1$ and $\Delta^2(s+\frac{1}{2}) \ll 1$.

(*a*) $\Delta^2(s+\frac{1}{2}) \gg 1$
We find

$$x_{s+1/2} = \frac{Q_{s+1/2}}{\Delta} = (s+\tfrac{1}{2})\left\{\left(1-\frac{1}{2\gamma}\right)+\frac{1}{\gamma}\left(\frac{\gamma}{\Delta^2(s+\frac{1}{2})^2}+\frac{1}{4}\right)^{1/4}\right\} \tag{42}$$

where s is an integer in the range

$$(N/2-\tfrac{1}{2}) \geqslant s \geqslant 0 \tag{43}$$

and γ is defined by (24). In the limit

$$(s+\tfrac{1}{2})^2\Delta^2 \gg 4\gamma \tag{44}$$

this reduces to

$$Q_{s+1/2} = (s+\tfrac{1}{2})\Delta + \frac{1}{(s+\frac{1}{2})\Delta}. \tag{45}$$

In table 2 we have listed the positive eigenvalues for $N = 3, 9$ and 19 when Δ takes the values $\Delta = 0{\cdot}1$, $0{\cdot}5$, $1{\cdot}0$, $2{\cdot}0$ and $10{\cdot}0$. It can be seen readily from this table that (45) gives a good approximation to the eigenvalues when (44) is satisfied.

In the opposite limit

$$(s+\tfrac{1}{2})^2\Delta^2 \ll 4\gamma \tag{46}$$

(42) reduces to

$$Q_{s+1/2} = \Delta(s+\tfrac{1}{2})\left(1-\frac{1}{2\gamma}\right)+\gamma^{-1/2}. \tag{47}$$

(*b*) $\Delta^2(s+\frac{1}{2}) \ll 1$
In this limit we obtain

$$x_{s+1/2} = \frac{Q_{s+1/2}}{\Delta} = (s+1)\left(1-\frac{\Delta^2}{\Delta^2+\pi^2}\right) \tag{48}$$

for s an integer in the range

$$(N/2-\tfrac{3}{2}) \geqslant s \geqslant 0. \tag{49}$$

The final root is given by

$$Q_{N/2} = (N+1)^{1/2} \tag{50}$$

which is equal to the square root of the total number of modes, as in the N even case. (50) is valid if

$$\Delta^2(N/2) \ll 1. \tag{51}$$

From table 2 we see that (50) gives a good approximation to the final roots in the cases where $\Delta = 0{\cdot}1$, $N = 3, 9$ and 19 (which satisfy (51)).

4. Connection with the results of Davidson and Kozak, and Weisskopf and Wigner

Before describing the time dependent properties it is convenient to discuss the connection between our approach, and that of other workers. Davidson and Kozak (1971) have considered the same model as we have, and have given an exact expression for $P_0(t)$ by calculating the probability amplitude. They used resolvent techniques similar to those used by the Brussel's school in master equation theory. The result they obtained was

$$P_0(t) = |A(t)|^2 \tag{52}$$

where

$$A(t) = -\frac{1}{2\pi i}\oint \frac{dz\, e^{-izt}}{z - \Sigma_\lambda |g_\lambda|^2/(z-\omega_{\lambda,0})} \tag{53}$$

(this is their equation (12) converted to our notation). The contour in (53) is parallel to the real axis and lies above all the singularities of the denominator. For a finite number of discrete modes, the singularities will all be poles, and we may evaluate (53) using the calculus of residues to obtain

$$A(t) = \sum_q e^{-iqt} \lim_{z\to q}\left(\frac{z-q}{z - \Sigma_\lambda |g_\lambda|^2/(z-\omega_{\lambda,0})}\right) \tag{54}$$

where q is a root of the equation

$$z - \sum_\lambda \frac{|g_\lambda|^2}{z-\omega_{\lambda,0}} = 0. \tag{55}$$

(55) is essentially our equation (7) for the eigenvalues Q written in terms of dimensional variables. The limit on the right hand side of (54) may be evaluated using L'Höpital's rule to give

$$A(t) = \sum_q \frac{e^{-iqt}}{1 + \Sigma_\lambda |g_\lambda|^2/(q-\omega_{\lambda,0})^2} \tag{56}$$

which together with (52) is essentially our result (8) and (9), so that our expressions are equivalent to those of Davidson and Kozak. These authors used (53) to discuss the behaviour of an atom interacting with an infinite number of modes of the electromagnetic field.

Attention should be drawn to the similarity between (53) and the expression obtained using conventional Wigner–Weisskopf theory (Louisell 1964, equation (5.80)). In the Wigner–Weisskopf approximation one essentially solves the equations of motion by considering only those transitions from an initial state with the atom in its excited state and no photons present to states in which there is one photon present and the atom is in its ground state. The rotating wave approximation retains only those terms in the Hamiltonian which connect these states (see the discussion in I) so that it is not surprising that the Wigner–Weisskopf approximation and the rotating wave approximation lead to essentially the same equations.

However, in the usual Wigner–Weisskopf theory a further approximation is made which leads to irreversible behaviour. This involves transforming the sum over modes in (53) to an integral, and then evaluating it approximately (Louisell 1964). This leads to the exponential decay

$$P_0(t) = e^{-\Gamma t} \tag{57}$$

where

$$\Gamma = 2\pi|g_\lambda|^2\rho(\omega)|_{\omega_0} \tag{58}$$

and $\rho(\omega)$ is the number of states per unit energy range for the field at ω.

For the model under consideration here, it is clear that

$$\rho(\omega_0) = \frac{1}{\delta} \tag{59}$$

and thus if the Wigner–Weisskopf approach is valid in our case, we should find that

$$P_0(\tau) \simeq \exp\left(-\frac{2\pi}{\Delta}\tau\right). \tag{60}$$

We will later compare (60) with the numerical solutions of our equations.

5. The time dependent properties

We have used an electronic computer to evaluate expressions (9) and (17) for $P_0(t)$ and $p_n(t)$ for various values of N and Δ. We first consider the case when $N = 4$, which corresponds to 5 field modes being present, one of which is on resonance with the atom. Figures 2, 3, 4, 5 and 6 show $P_0(\tau)$ as a function of the dimensionless time $\tau = |g|t$ for $\Delta = 0{\cdot}1$, $0{\cdot}5$, $1{\cdot}0$, $2{\cdot}0$ and $10{\cdot}0$ respectively.

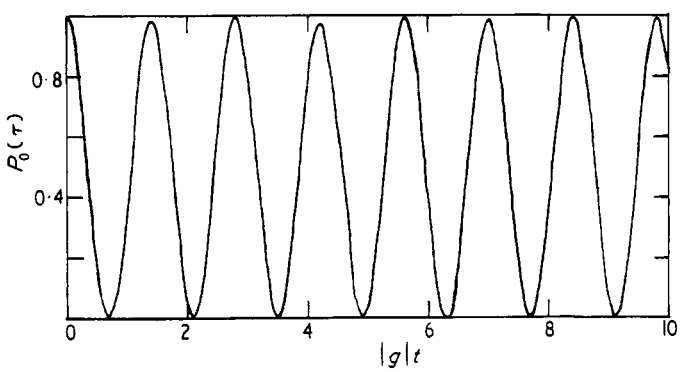

Figure 2. P_0 as a function of $\tau = |g|t$ for the 5 mode case with $\Delta = 0{\cdot}1$.

Figure 2 shows how closely $P_0(\tau)$ approximates to a periodic function for $\Delta = 0{\cdot}1$. This may be understood by referring to table 1 where it may be seen that the final eigenvalue $Q_{N/2}$ is much larger than any of the other eigenvalues, and also much larger than $\frac{1}{2}N\Delta$. Making use of the latter inequality in (16) for $|B_Q(0)|^2$ it is readily seen that

$$|B_{Q_{N/2}}(0)|^2 \simeq 1 \gg |B_{Q_n}(0)|^2 \tag{61}$$

for $n \neq N/2$. This situation will always obtain when $\frac{1}{2}N\Delta^2 \ll 1$. Hence from (9)

$$P_0(\tau) \simeq \cos^2(Q_{N/2}\tau) \tag{62}$$

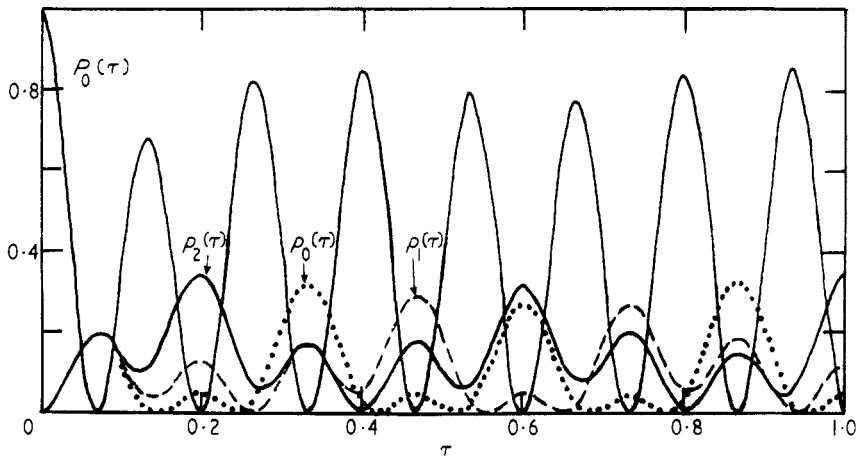

Figure 3. P_0 (full curve), p_0 (dotted curve), $p_{\pm 1}$ (broken curve) and $p_{\pm 2}$ (full curve with small amplitude) as functions of τ for the 5 mode case with $\Delta = 0{\cdot}5$.

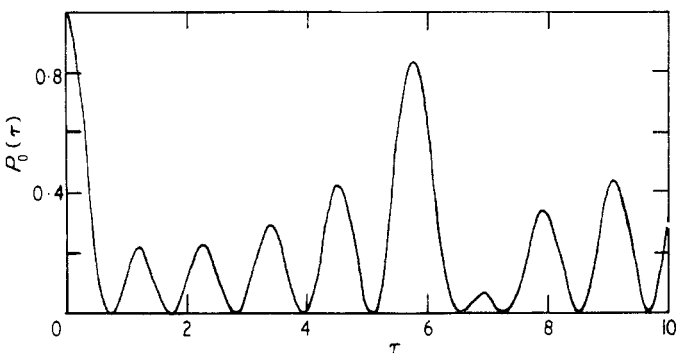

Figure 4. P_0 as a function of τ for the 5 mode case with $\Delta = 1$.

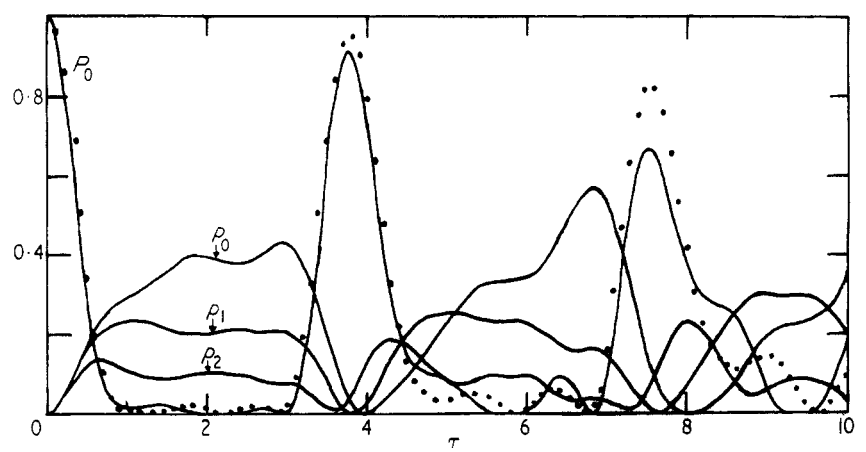

Figure 5. $P_0, p_0, p_{\pm 1}$ and $p_{\pm 2}$ as functions of τ for the 5 mode case with $\Delta = 2$. Also shown is $P_0(\tau)$ for the 4 mode case with $\Delta = 2$ (dotted curve).

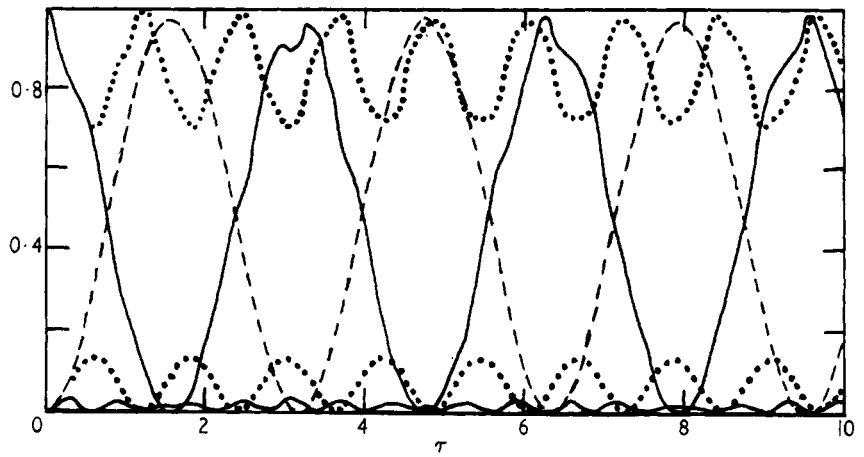

Figure 6. P_0 (full curve), p_0 (broken curve) and $p_{\pm 1}$ (full curve with small amplitude) as functions of τ for the 5 mode case with $\Delta = 10$. Also shown are $P_0(\tau)$ and $p_{\pm 1/2}(\tau)$ for the 4 mode case with $\Delta = 10$ (dotted curves). P_0 is the upper of the two curves.

and the period of the oscillations is

$$T = \frac{\pi}{Q_{N/2}}. \tag{63}$$

(63) predicts the period quite accurately within its range of validity.

In figure 3 for $\Delta = 0{\cdot}5$, $P_0(\tau)$ has the appearance of a modulated sine wave. In this case the condition $Q_{N/2} \gg \frac{1}{2}N\Delta$ is not strictly satisfied, and the contribution from $|B_{Q_{N/2}}(0)|^2$ is not so dominant, but the period is still given approximately by (63). Also shown in figure 3 are $p_{\pm 2}(\tau)$, $p_{\pm 1}(\tau)$ and $p_0(\tau)$ for $\Delta = 0{\cdot}5$. In figure 4, where $\Delta = 1$, the modulated sine wave behaviour is becoming less apparent, and in figure 5, where $\Delta = 2$, it has disappeared. In these cases, many $|B_Q(0)|^2$ contribute significantly to $P_0(\tau)$. In figure 5, the behaviour of $P_0(\tau)$ consists of a rapid decay, followed by a few oscillations of small amplitude, and then a sudden and steep rise to a value near to unity. In addition to $p_{\pm 2}(\tau)$, $p_{\pm 1}(\tau)$, $p_0(\tau)$ we have plotted $P_0(\tau)$ for $N = 3$ (corresponding to 4 modes) for the same value of Δ. This is shown as a dotted curve. It is apparent that the behaviour is qualitatively very similar to that for $N = 4, \Delta = 2$ so that whether there is a mode on resonance with the atom or not makes very little difference, at least for $\Delta \lesssim 2$. According to the discussion in I, we would expect to see qualitative differences between the cases N even or N odd if Δ is made sufficiently large.

The cases for which $\Delta = 0{\cdot}1$ and $0{\cdot}5$ correspond to strong coupling between the atom and the field modes, those for which $\Delta \sim 1$ correspond to intermediate coupling, and that case for which $\Delta = 10$ corresponds to weak coupling. The latter case is shown in figure 6, where $P_0(\tau)$ now has the appearance of a distorted cosine curve. This is because the atom effectively interacts strongly with only one mode, that with which it is on resonance. This interpretation is supported by the appearance of $p_0(\tau)$, which is approximately that of a sine wave. The amplitude of $p_0(\tau)$ is about 0·98, that of $p_{\pm 1}(\tau)$ is about 0·03, and that of $p_{\pm 2}(\tau)$ is about 5×10^{-3}, too small to be shown in figure 6.

We have considered the case $N = 3, \Delta = 10$, and we have plotted $P_0(\tau)$ and $p_{\pm 1/2}(\tau)$ in figure 6 for comparison with the $N = 4, \Delta = 10$ case. The readily apparent qualitative differences between the curves for $P_0(\tau)$ in these two cases are due to the fact that in

the $N = 3$ case there is no field mode which has an energy close to that of the atom. This property also accounts for the small amplitude of the $p_{\pm 1/2}(\tau)$ curve as compared with the $p_0(\tau)$ curve for $N = 4$.

The plots of $p_{\pm 2}(\tau)$, $p_{\pm 1}(\tau)$ and $p_0(\tau)$ shown in figures 3, 5 and 6 demonstrate how the energy is distributed between the atom and the modes. Consider first the distribution over the field modes. For $\Delta \gtrsim 1$ the energy mostly resides in those modes closest in energy to the atomic energy (as one might expect) but for $\Delta \ll 1$ (the case of strong interaction) the energy tends to be more evenly distributed. In the case $\Delta = 10$, practically all the energy resides in the mode on resonance. As regards the average energy stored in the atom, this is seen to be largest ($\sim \frac{1}{2}$) when Δ is very small and very large, and to reach a minimum in the region $\Delta \sim 1$. When N is odd and Δ is large (as in figure 6) it is clear that a considerable fraction of the energy always resides in the atom.

Let us now consider the 21 mode case ($N = 20$) for the same values of Δ. We have not plotted the case $N = 20$, $\Delta = 0{\cdot}1$ as the behaviour is very similar to that shown in figure 2 for $N = 4$, $\Delta = 0{\cdot}1$. The period is now shorter (as given by (63)) and the height of the peaks not quite so close to unity, but $P_0(\tau)$ is still well approximated by a periodic function. The case $N = 20$, $\Delta = 0{\cdot}5$ shown in figure 7 shows marked differences from

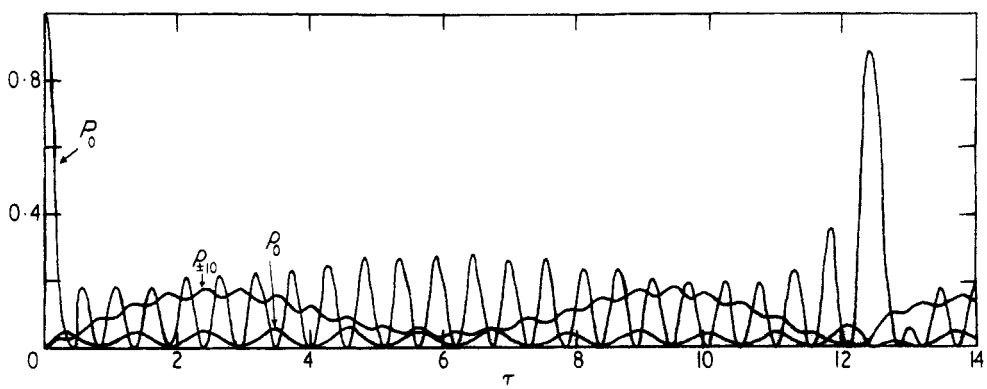

Figure 7. P_0 as a function of τ for the 21 mode case with $\Delta = 0{\cdot}5$. Also shown are $p_0(\tau)$ and $p_{\pm 10}(\tau)$.

the case $N = 4$, $\Delta = 0{\cdot}5$. Now the height of most of the peaks is considerably less than one, but every so often there is a sudden rise to a value close to unity. It is appropriate at this stage to comment on a general property of $P_0(\tau)$. The term $P_0(\tau)$ is equal to unity at $\tau = 0$ and will be equal to unity again at a later time if we can find a value of τ which simultaneously satisfies

$$Q_i \tau = 2n_i \pi \tag{65}$$

for all the roots Q_i where n_i is an integer. This may be inferred from (9). However, because the Q_i are in general irrational numbers no value of τ can be found which satisfies (65) exactly, although values can be found which satisfy it approximately. $P_0(\tau)$ (and the $p_n(\tau)$) belong to the set of almost periodic functions (Bohr 1947). For those values of τ which do satisfy (65) approximately, $P_0(\tau)$ will be of the order of unity. In this event, a Poincaré recurrence is said to have occurred.

These recurrence effects become even more pronounced when we consider the case $N = 20$, $\Delta = 1$ shown in figure 8. After a sharp decay, $P_0(\tau)$ undergoes oscillations of

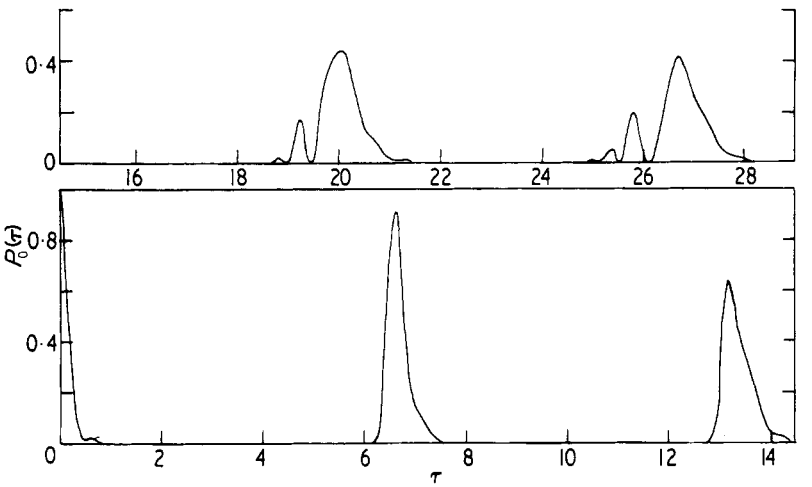

Figure 8. P_0 as a function of τ for the 21 mode case with $\Delta = 1$.

very small amplitude (too small to be apparent in figure 8) for a considerable time, until suddenly $P_0(\tau)$ increases to a value near to one, and then decays again. In this example the first few Poincaré recurrences are very well defined. We have plotted $P_0(\tau)$ over a larger time scale in this case to show how the single Poincaré peaks gradually break up into several peaks. As we increase Δ to $\Delta = 2$ in figure 9, the Poincaré recurrences are still evident, but they are no longer as sharp.

We have calculated $P_0(\tau)$ for the case $N = 20, \Delta = 10$, but the behaviour is practically identical to the case $N = 4$, $\Delta = 10$. Because the curves for $N = 4$ and $N = 20$ would be indistinguishable in an ordinary plot, we have not given a separate graph of the $N = 20$ case. This similar behaviour is striking confirmation of the argument that when the field modes are well separated in energy from the atomic energy, they do not interact effectively with the atom.

This property may be deduced from our equations by substituting the approximate expressions (25) and (28) for the eigenvalues Q into (16) for $|B_Q(0)|^2$, and then taking the

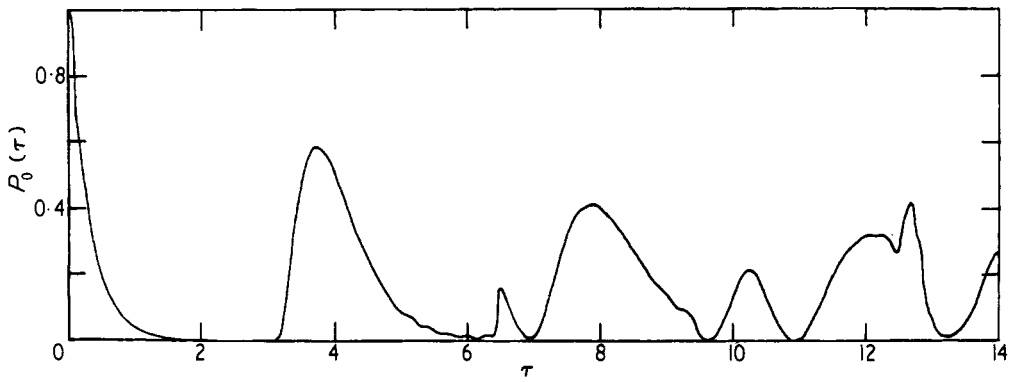

Figure 9. P_0 as a function of τ for the 21 mode case with $\Delta = 2$.

limit $\Delta \to \infty$. One finds that

$$|B_{Q_s}(0)|^2 \to \frac{1}{1+\Delta^2 s^2} \to 0 \qquad Q_s \neq 0 \tag{66}$$

and

$$|B_0(0)|^2 \to \frac{1}{1+\gamma} \to \frac{1}{2} \qquad Q_s = 0. \tag{67}$$

Substituting (66) and (67) into (9) and (17) one finds that

$$P_0(\tau) \sim \cos^2\tau \tag{68}$$

and

$$p_n(\tau) \sim \begin{cases} \sin^2\tau & n = 0 \\ \dfrac{\text{trigonometric function of } \tau}{\Delta^2 n^2} & n \neq 0 \end{cases} \tag{69}$$

even for N very large. (66) to (69) apply when N is even. If N is odd, we find similarly that the following limits apply as $\Delta \to \infty$:

$$P_0(\tau) = 1 - \frac{4}{\Delta^2} \sum_{r=-N/2}^{+N/2} \frac{1-\cos(r\Delta\tau)}{r^2} + O\left(\frac{1}{\Delta^4}\right) \tag{70}$$

and

$$p_{\pm r}(\tau) = \frac{4}{r^2\Delta^2} \sin^2(\tfrac{1}{2}r\Delta\tau) + O\left(\frac{1}{\Delta^4}\right) \tag{71}$$

where we have set $r = n + \frac{1}{2}$ so that r is half-integral. If we retain only the first term ($r = \frac{1}{2}$) in the sum in (70) and take $r = \frac{1}{2}$ in (71) we obtain the relations given in I for the two mode case (I 51). (70) and (71) account quite well for the curves given in figure 6

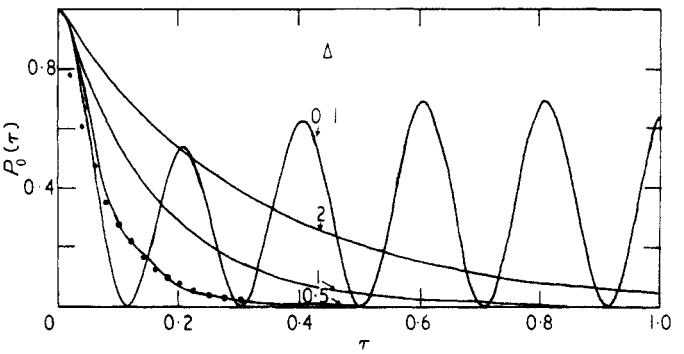

Figure 10. P_0 for the 201 mode case with $\Delta = 0{\cdot}1, 0{\cdot}5, 1$ and 2 as functions of τ. The dots are points on the curve $\exp(-4\pi\tau)$. Note that the time scale in this diagram is considerably shorter than in the other diagrams.

for $N = 3, \Delta = 10$. It is clear that the sum in (70) exists (and converges rapidly) as the limit $N \to \infty$ is taken so that one would expect little difference between the behaviour shown in figure 6 for $N = 3$ and that for larger values of N (and the same value of Δ).

Finally we consider the situation when $N = 200$. In figure 10 we have plotted $P_0(\tau)$ for the cases $\Delta = 0{\cdot}1, 0{\cdot}5, 1$ and 2. It is observed that the oscillatory behaviour persists in the $\Delta = 0{\cdot}1$ case even when we are dealing with 201 modes. (The period is still given approximately by (63) even though $\frac{1}{2}N\Delta^2 = 1$.) In the $\Delta = 0{\cdot}5$ case, the behaviour is now that of a steady decay to a value near zero, after which $P_0(\tau)$ oscillates with very small amplitude (of the order of 10^{-5}). Similar behaviour occurs in the $\Delta = 1$ and $\Delta = 2$ cases.

We will now compare these exact results with the approximate expressions (60) given by the Wigner–Weisskopf theory, which we might expect to hold for times neither too long nor too short for large values of N. It is clear that it does not hold even approximately for the $\Delta = 0{\cdot}1$ case, but the $\Delta = 0{\cdot}5$ case shows better agreement. In figure 10 we have plotted various points on the curve $\exp(-4\pi\tau)$ for comparison with the exact $\Delta = 0{\cdot}5$ curve, and it may be seen that although the exact and approximate expressions deviate appreciably for short times, the agreement for times greater than about $\tau = 0{\cdot}1$ is reasonably good. (Of course, (60) cannot account for the Poincaré recurrences and small amplitude oscillations which are characteristic of the exact solutions.)

For the $\Delta = 1{\cdot}0$ and $\Delta = 2{\cdot}0$ cases the agreement between the approximate and exact expressions is even better (typically to within a few per cent over most of the range shown in figure 10). We have not plotted (60) for these two cases as the curves would not be readily distinguishable from the exact curves. Physical continuity and time reversal symmetry require that the exact solution has zero gradient at $\tau = 0$ whereas (60) predicts a gradient of $-\Gamma$. The function $P_0(\tau)$ in figure 9 for $N = 20, \Delta = 2$ is also well approximated by (60) in the range $0{\cdot}1 \geqslant \tau \geqslant 3{\cdot}0$. From this discussion it is apparent that the Wigner–Weisskopf approach gives a reasonable approximation to our exact results for $P_0(\tau)$ if $\Delta \sim 1$ or 2 and $N\Delta \gtrsim 40$.

It is interesting to note that our model (which is a purely dynamical one) shows a statistical mechanical type of behaviour for those values of the parameters for which the Wigner–Weisskopf theory is valid: after an initial, approximately exponential decay the atom settles to an 'equilibrium' state ($P_0(\tau) \sim 0$) where it then undergoes oscillations of small amplitude (typically of the order of 10^{-5}–10^{-6} or smaller—too small to be shown in figure 10) which corresponds to the fluctuations of a system in statistical equilibrium. After a relatively long time interval, $P_0(\tau)$ suddenly undergoes a rapid transition to a value close to its initial value (as required by dynamics), and then decays again. (For the case $N = 200, \Delta = 1$ for example, the first appreciable fluctuation occurs at $\tau \simeq 6{\cdot}5$, when $P_0(\tau)$ obtains a value of about 0·56. This is practically the same value of τ for the first Poincaré recurrence for the case $N = 20, \Delta = 1$ (figure 8) but then the maximum value of $P_0(\tau)$ was about 0·92.) One may thus regard the atom as interacting with a peculiar type of reservoir composed of the electromagnetic field modes.

Acknowledgments

The author is extremely grateful to Miss Cathleen McCollum who wrote the computer programs. This research was supported by The Advanced Research Projects Agency of the Department of Defense and was monitored by the Office of Naval Research under Contract No N00014-69-C-0035.

References

Bohr H 1947 *Almost Periodic Functions* (New York: Chelsea)
Davidson R and Kozak J J 1971 *J. math. Phys.* **12** 903–17
Louisell W M 1964 *Radiation and Noise in Quantum Electronics* (New York: McGraw-Hill)
Swain S 1972a *J. Phys.* A: *Gen. Phys.* **5** L3–6
—— 1972b *Phys. Lett.* **39A** 143–4
—— 1972c *J. Phys.* A: *Gen. Phys.* **5** 1587–600